Study on Thermocapillary Convection in an Annular Liquid Pool

Li Duan, Qi Kang, Di Wu, Li Zhang, Di Zhang, Huan Jiang, Chu Zhang, Yongli Yin and Wenrui Hu

Abstract Thermocapillary convection is an important content in the study of microgravity fluid physics. It is not only the problem of fluid physics mechanism such as convection stability, but also closely related to spacecraft flow control, efficient heat transfer, etc., and has direct guiding significance for material growth processes such as floating zone method and Czochralski method. This chapter mainly introduces the research status of thermocapillary convection about an annular liquid pool, the scientific experiment and partial analysis results carried out by the project group in the early stage, and the development of space experimental payload, space experiment and preliminary experimental results about the annular liquid pool from SJ-10 mission.

Keywords SJ-10 mission · Space experiment · Microgravity fluid physics · Thermocapillary convection · Annular liquid pool · Convection instability · Chaos · Bifurcation · Transition routes · Volume ratio effect

1 Introduction

Among many new energy sources, solar energy is the best energy choice known to mankind for some advantages such as renewability, cleanliness, wide applicability, and economical efficiency. Solar photovoltaic industry is based on silicon materials. The monocrystalline silicon is the first discovered, studied and applied. It is still

L. Duan · Q. Kang (✉) · D. Wu · L. Zhang · D. Zhang · H. Jiang · C. Zhang · W. R. Hu
Key Laboratory of Microgravity (National Microgravity Laboratory) Institute of Mechanics, Chinese Academy of Sciences, No.15 Beisihuanxi Road Haidian District, Beijing 100190, China
e-mail: kq@imech.ac.cn

L. Duan · Q. Kang · W. R. Hu
School of Engineering Science, University of Chinese Academy of Sciences, No. 19(A) Yuquan Road, Shijingshan District, Beijing 100049, China

Y. L. Yin
Astronaut Research and Training Center, Youyi Road, Haidian District, Beijing 100094, China

W. R. Hu and Q. Kang (eds.), *Physical Science Under Microgravity: Experiments on Board the SJ-10 Recoverable Satellite*, Research for Development,
https://doi.org/10.1007/978-981-13-1340-0_5

one of the most important materials for solar cells. Monocrystalline silicon, a single crystal of silicon, is a kind of semiconductor material with good performance. There are different crystal growing methods, including Czochralski (Cz) method, float zone method, and epitaxial method. The monocrystalline silicon by Cz method is the most widely used material. That is the most important method for the growth of semiconductor crystals. It is divided into seven stages including filling material, melting material, contacting the seed crystal with the melt, pulling the thin neck, pulling the shoulder, pulling the body and pulling the end zone. The technology of pulling single crystals by seeded crucible melts was firstly used in 1918 by J. Czochralski to grow metallic crystals. It is called Cz method. Cz method uses the principle of solidifying crystallization of the melt to establish a temperature field, form a certain degree of super-cooling on the solid-liquid interface, and ensure the other regions not overheated at the same time; the melt is crystallized on the seeded crucible, and the rod like crystal is formed with the rising of the pulling rod. Therefore, in Cz method, the control of heat transfer is the key for the successful growth of crystals. As a result, to establish an appropriate temperature field is a very important condition to grow high quality crystals. The flow in the melt is closely related to the temperature field, and the change in the flow state will influence the distribution of molten materials and impurities as well as the performance of the crystal.

During the crystal growing process by Cz method, momentum transport (distribution of fluid velocity), energy transport (distribution of temperature) and mass transport (distribution of melting concentration) are involved. When the crystal grows, it melts and cools at the same time, and there is a temperature gradient on the crystal surface. This kind of temperature distribution, on the one hand, causes the difference in density of silicon melt at the wall and the core of the crucible, and causes buoyancy convection, thus, the silicon melt with high density and low temperature near the core is pressed to the bottom of the crucible, and then it is heated up at the bottom and rises up along the wall of the crucible, forming a convection cycle; on the other hand, thermocapillary convection driven by the gradient in surface tension on the free surface, which is also called Marangoni flow, is also an important factor leading to the decrease in uniformity and unidirectional property of the temperature field of melt as well as the crystal. In addition, with the forced convection caused by the crystal rotation, during the practical process of crystal growth, variable factors act on the melt and make the melt flow very complicated, leading to the un-uniformity in properties of the crystal, producing mechanical stress and dislocation, and as a result, affecting the quality of the crystal (Fig. 1).

The instability of flow field has attracted more and more attention since it was firstly discovered. In the last century, many scientists have simulated the flow in the Cz furnace, and analyzed the change rule of the configuration of crystallization interface. From the whole view of the work done, natural convection in the melting flow takes the dominating role, and forced convection takes the secondary role [2–5].

Convection is a common physical phenomenon in nature. In the gravitational field on the ground, in a fluid region with warmer fluid on the bottom and cooler fluid on the top, buoyancy will drive the warmer fluid up to form a convection, and this is called buoyancy convection. On the liquid free surface in an open container, if there

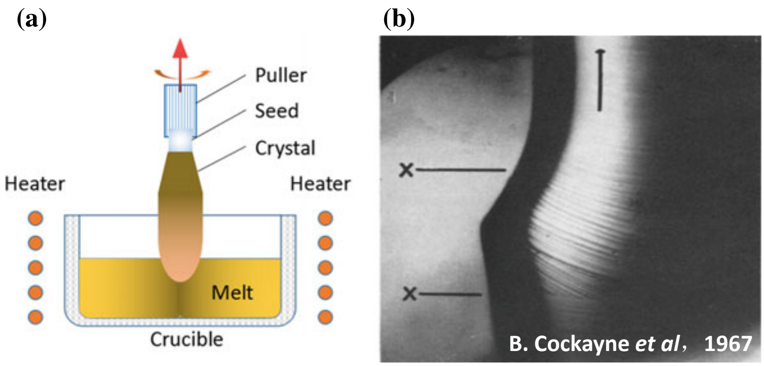

Fig. 1 The physical model of Cz method (left) and the slice map of crystal with striations defects (right). Reprinted from Ref. [1], copyright 1967, with permission from Springer Nature

is a temperature gradient on the liquid surface, there will be a gradient of surface tension. Because the surface tension is inversely proportional to the temperature, under the effect of surface tension gradient, the fluid on the free surface will flow from the hot end to the cold end. In addition, because of viscosity and conservation of mass of the fluid, the free surface flow will drive the flow in the whole flow field. As early as in 1686, Heyde has observed the movement of camphor fragments on the free surface of olive oil. Due to various factors such as temperature and concentration, there is always difference in the distribution of surface tension on the liquid free surface, thus there exists gradient of surface tension. The fluid on the liquid surface usually moves to the area with higher surface tension, thus the convection is formed. The camphor fragments used as tracer particles showed the phenomenon of convection. Afterwards, the convection driven by the gradient of surface tension is called Marangoni convection, among which, the convection caused by un-uniformity in surface tension due to un-uniformity in surface temperature is called thermocapillary convection. Buoyant effect cannot be neglected in the study of thermocapillary convection in the gravity environment on the ground. The fluid flow is the coupled flow of thermocapillary convection and buoyant convection, so it is usually defined as buoyant-thermocapillary convection. People gradually realized that, under some extreme conditions, such as in the microgravity environment in space or in a small scale fluid system, the influence of gravity will be greatly weakened, and thermocapillary convection is the dominant factor in the process of natural convection [6–8].

More and more frequent aerospace activities and opening of the space station provide people many opportunities and resources to carry out research on pure thermocapillary convection. From the formation mechanism of thermocapillary convection, it is a nonlinear result of coupling effects of flow field and temperature field as well as mechanical movement and thermal movement. With the change of control parameters, viewed from the change of state of fluid, it may transit from original two-dimensional basic flow or axisymmetric flow to three-dimensional full field flow, from steady convection to unsteady convection or even oscillatory convection, from periodic oscillatory convection to chaos, and at last, under a certain condition, it may transit from laminar flow to turbulent flow as many other classic flow models do. Many problems in this process need to solve, so thermocapillary convection and its instability property are still open problems.

At present, the study on chaos and turbulence of fluid is a long-term and challenging project. For an unknown nonlinear system, the chaos phenomenon is ubiquitous, and the chaos theory is possible to explain the transition process of fluid from simple laminar flow to complex turbulent flow. However, there are few related reports on chaos study and analysis about experimental measurements of a nonlinear system. Therefore, numerical analysis on chaotic dynamics to the nonlinear model of annular liquid pool with Cz method is a very good try out.

SJ-10 recoverable satellite provides us a very good experimental condition under microgravity environment in space, and gives us the opportunity to carry out deep study on the phenomenon and mechanism of pure thermocapillary convection.

2 Research Status on Thermocapillary Convection

The instability of thermocapillary convection was first brought up by Smith and Davis [9]. They performed linear stability analysis on thermocapillary convection in the infinite horizontal thin liquid layer with a free surface driven by the horizontal temperature gradient, and discovered two kinds of instability, stable axial rolling cells and hydrothermal waves. They suggest that the critical Marangoni number (Ma_c) and the critical wave number are determined by Prandtl number (Pr) of the fluid. Generally, Marangoni number Ma characterizes the strength of thermocapillary convection; and Prandtl number characterizes the momentum exchange and the heat exchange in the fluid flow. Their definition is as Eqs. (1) and (2).

$$Ma = \frac{\sigma_T \Delta T L}{\rho \nu \kappa} \tag{1}$$

$$Pr = \frac{\nu}{\kappa} \tag{2}$$

where, ν is the kinematic viscosity, ρ is the density of fluid, κ is the thermal diffusivity, σ is the surface tension, σ_T is the temperature coefficient of surface tension, and ΔT is temperature difference.

Later researchers studied stability of thermocapillary convection and buoyant-thermocapillary convection under various conditions with this method [10–19], obtained critical conditions of flow transition process, analyzed influences of various factors on this process, and determined various possible flow models after destabilization. Hydrothermal waves are widely used in explaining the transition mechanism of thermocapillary convection from quasi-steady flow to oscillatory flow. With the perturbation theory, we can get perturbation solutions by solving eigenvalue equations and boundary condition equations, and for the basic state flow, we can get travelling wave solutions for perturbations of hydrothermal waves. This indicates the transition from steady single cell convection to oscillatory convection of hydrothermal waves. Generally, the relationship between the critical *Ma* number and *Pr* number can be obtained through calculation.

For thermocapillary convection, as a fluid mechanics system, its oscillation characteristics and the whole transition process from laminar flow to turbulent flow must be of great interest for theoretical research. On the other hand, many applications of thermocapillary convection should avoid the occurrence of oscillation. With the development of manned space activities, people have a great interest in the space material processing, especially the container free process for growing crystal in space, and try to realize the material production by pure distribution process by using the property of almost disappeared buoyancy effect in the microgravity environment, which is the aspirational material producing environment for mankind. However, in fact, in the microgravity environment, some secondary effects such as surface tension take the dominant role, and thus thermocapillary convection is prominent. Therefore, the study on thermocapillary convection has significant meanings in both theory and applications. Kang and Duan et al. [20–25] studied transition problems of thermocapillary convection in detail. They discovered a few transition routes including quasi-periodic transition, period-doubling bifurcation, quasi-periodic transition with tangent bifurcation, and period-doubling bifurcation with tangent bifurcation, and also found the laws for the occurrence of various transition routes. Tang, Li, and Hu et al. [26, 27] discussed transition routes of thermocapillary convection in the liquid bridge model of half-floating zone through numerical simulations, found the period-doubling bifurcation, and proved that the period-doubling bifurcation process of thermocapillary convection satisfies Feigenbaum general theorem. The quasi-periodic transition with tangent bifurcation and the period-doubling bifurcation with tangent bifurcation are relatively uncommon. There are abundant contents in the research on transition routes, and more models need to be further studied in this area.

Because the annular liquid pool is geometrically similar to the model for crystal growth by Cz method, the research on it has been widely concerned. The experimental study on thermocapillary convection in an annular pool was firstly carried out by Kamotani et al. [28]. 2cSt silicone oil with *Pr* number of 27 was used in their experiments, and the diameter of the liquid pool was 3.98 cm, 4.78 cm and 5.87 cm respectively. The oscillation phenomenon of thermocapillary convection was observed. After the onset of oscillation, the flow field turns into a non-axisymmetric three-dimensional structure; the velocity of surface flow is greatly higher than the velocity of inverse flow in the lower part of the fluid; the curve of temperature oscillation is approximately sinusoidal, and if *Ar* is fixed, the critical temperature difference for the onset of thermocapillary convection is not related to the radius of the liquid pool, so oscillation cannot be simply characterized by *Ma* number alone; surface thermal images show the periodic change of temperature oscillation, indicating that the intensity of convection on the radial plane is unstable and fluctuating.

In 1992, Kamotani and Ostrach et al. [29–31] finished the first experiment under microgravity condition, observed stable thermocapillary convection, and numerically studied the axisymmetric flow in steady state. The experimental fluid was 10cSt silicone oil, the diameter of the liquid pool was 10 cm, and the depth was 5 cm. Two sets of heating systems were used. One was the laser heating system with the laser diameter of 0.5–3.0 cm, and the other was the electric film heating system with the film diameter of 1.11 cm. By using the flow visualization technology (PTV), they observed flow fields with different heating methods and different shapes of free surface, and obtained 18 sets of experimental results, which were in good agreement with corresponding numerical results. The obtained $Ma = 3.1 \times 10^5$, was 5 times as high as that obtained in the ground experiment, but the oscillation had not been observed yet.

In 1995, Kamotani and S. Ostrach [32–37] finished the second experiment under microgravity condition in USML-2 space laboratory. The experimental fluid was 2cs silicone oil with $Pr = 27.33$, the diameter of the liquid pool was 1.2 cm, 2.0 cm and 3.0 cm respectively $Ar = 1$, $Ma < 6 \times 10^5$, and the temperature of the wall was 14 °C. When Ma number is high enough, the driven force of thermocapillary convection is mainly concentrated at the hot zone and the cold zone, and the oscillation phenomenon is closely related to the flow in the hot zone. The flow fields and the temperature fields of steady flow as well as oscillatory flow were observed, and the critical oscillation conditions were determined in this space experiment. The flow field was observed qualitatively, and the experimental result of thermocapillary convection in the liquid pool with 1.2 cm in diameter was in agreement with the result of ground experiments under 1-g condition. This indicates that the influence of gravity can be neglected in experiments with equipment equal to or smaller than this size. The surface deformation in the oscillation was also observed in the experiment, and a surface deformation parameter was defined. This parameter can well indicate the occurrence of oscillation, and when the free surface is very curved or the liquid layers very shallow, the oscillation will be delayed. The influence of heating rate on critical conditions was studied too. It turns out that the critical temperature difference is not related to the heating rate. Isotherms obtained by the thermal infrared imager discovered the change in temperature field on the surface during the oscillation process; the 2-earlobe oscillation mode was found in all experiments, and as the temperature difference was further increased, the pulsating pattern of 2-earlobe and 3-earlobe appeared. This indicates that, in an oscillation period, convection with fluctuating intensity will occur in different areas of the free surface. Later on, more experimental studies and numerical simulations about oscillatory flow in an annular pool have been completed by Ostrach et al. The silicone oil with Pr number of 27 was still used in their experiments, and the flowing states in an annular liquid pool were studied with the consideration of buoyant effect.

In 2001, Renaud et al. [38] experimentally and numerically studied nonlinear thermocapillary convection of the fluid with large Pr number in an annular pool, elaborated the oscillation characteristics of thermocapillary convection, and obtained distributions of the flow field and the temperature field. The results show that, oscillating thermocapillary convection is related to the capillary Re number; when the oscillation begins, it is in the standing wave form, and with the increase of acting force, it transforms into the travelling wave form; the number of hydrothermal waves depends on geometric parameters, and the mechanism of oscillation starting is related to fluid inertia, surface tension and buoyancy.

In the past decades, theoretical analyses and experimental studies on thermocapillary convection in various geometric structures have been completed, and transition processes of thermocapillary convection and various flow structures have been discovered. From 1990s to 2004, Sim and Schwabe et al. reported results of a series of three-dimensional numerical simulations on thermocapillary convection of fluids with medium *Pr* number in annuli [39, 40] as well as that of fluids with low *Pr* number in the annular shallow pool and the Cz structure shallow pool [41, 42]. They verified the existence of flow transitions and various oscillation modes. In recent years, people carried out further in-depth study on thermocapillary convection in the annular pool. In 2004, Sim et al. [43] studied axisymmetric thermocapillary convection with interface deformations in the open cylindrical annular pool. In this two-dimensional model, there is only steady convection no matter whether the interface deforms and how large *Re* number is. Therefore, even with large *Re* number and capillary number *Ca*, free surface deformations will not lead to oscillatory axisymmetric convection, so the deformed free surface is not the reason why the flow transits into oscillatory axisymmetric convection. When the free surface is convex at the cold wall and concave at the hot wall, there are two peaks if *Re* number is small and more waves if *Re* number is large. The heat dissipation on the free surface leads to more intensified convection when the *Bi* number is high, so obviously, the convection depends on the curvature of free surface. In addition, they compared thermocapillary convection in the cylindrical liquid bridge with that in the annular liquid pool [44]. These two models are based on the physical models for two methods of crystal growth technology, Cz method and floating-zone method, respectively. They also discussed dynamic free surface deformations in the axisymmetric model, and obtained results that were in agreement with the documentary [43]. That is, within a certain range of parameters, there is only steady convection in the axisymmetric model no matter how large *Re* number is, well, when *Re* number exceeds a certain critical value, the generated three-dimensional oscillatory flow depends on the aspect ratio (depth to diameter), *Pr* number and the melt volume *V*.

The earlier studies on restraining thermocapillary convection include: applying a magnetic field to the conductive melt, vibrating the wall to generate a flow field to restrain the surface flow, or injecting air parallel to the surface directly. These techniques are all attempted to reduce *Ma* number in order to weaken the fluctuation. The defect of these methods is that, due to the damping effect of ground state convection, the weakening of global mixing capacity results in macro segregation of chemical components. A way of improvement is to focus on instability of thermocapillary convection. Since the temperature of free surface determines the instability of flow, it is possible to change oscillation by changing temperature. Thus, the method of weakening fluctuations by changing the instability without changing the flow state is useful to improve the uniformity of single crystal growth no matter macroscopically or microscopically.

Schwabe et al. [45, 46] experimentally studied buoyant-thermocapillary convection in the annular liquid pool with inner and outer radius of 20 mm and 40 mm respectively and depth 2.5–20 mm by heating the outer wall and cooling the inner wall. It is found in their experiments that, the flow is steady multicellular flow under a small horizontal temperature difference. With the increase of temperature difference, the flow will lose its stability and show hydrothermal waves at first, and then, as the temperature difference is further increased, more complicated oscillatory flow will occur. In 2006, Schwabe and Benz et al. reported results of a set of successful experiments on thermocapillary convection in an annulus on the satellite FOTON-12 of Russia [47, 48]. In the experiments, the outer wall was heated and its radius was 40 mm, the inner wall was cooled and its radius was 20 mm, and the depth of the annulus was $d = 2.5$–20 mm. The experimental results show that, the flow is steady multicellular flow under a small horizontal temperature difference; as the temperature difference is increased, the flow will lose its stability and transits into hydrothermal waves first, then, as the temperature difference is further increased, more complicated oscillatory flow will occur. The results also show that, as the thickness of liquid layer increases, the number of flow cells in the multicellular structure decreases. The results of later numerical simulations are in agreement with the results of experiments.

Li et al. and Shi et al. carried out in-depth studies on thermocapillary convection of silicon melt in the annular shallow pool. In 2003, Li et al. [49] carried out a series of unsteady two-dimensional numerical simulations on thermocapillary convection in the annular liquid pool with the horizontal temperature gradient under the microgravity condition by the finite volume method. The outer wall of the annular liquid pool was heated and its radius was 40 mm, the inner wall was cooled and its radius was 20 mm, and the depth of the liquid pool was 3–14 mm. 0.65cSt silicone oil ($Pr = 6.7$) was used as the experimental fluid. The numerical results are depicted as a stability chart by the aspect ratio Ar (the ratio of depth to groove width) and thermocapillary Reynolds number Re, and show that time-dependent movements will only occur when the aspect ratio is larger than a certain value (about 2.29). In 2004, Li et al. [50] carried out unsteady three-dimensional numerical simulations on thermocapillary convection of the melt with low Pr number in the shallow pool of Cz structure under the action of horizontal temperature gradient by the finite difference method, and verified the existence of hydrothermal waves and the second transition in the flow.

In 2006, Shi et al. [51] calculated the critical conditions for the generation of hydrothermal waves in the annular pool under the normal gravity condition and the microgravity condition respectively. They analyzed characteristics of thermocapillary convection of the silicon melt and hydrothermal waves when the outer wall was heated and the inner wall was cooled. Research shows that the hydrothermal wave is one of the forms of unsteady flow in the annular pool, and its wave number and angular velocity change with the change of Ma number. When Ma number is small, a single group of hydrothermal waves spread to the entire region gradually with the increase of computation time, but when Ma number is increased, multiple groups of hydrothermal waves propagating in different azimuthal directions will exist at the same time, in addition, the curvature of temperature curve of the hydrothermal wave is large near the hot wall. In 2007, Peng et al. [52] studied three-dimensional buoyant-thermocapillary convection of silicone oil in the annular pool. Their results show that, there are three types of flow patterns when Ma number is large: when the liquid pool is shallow ($d = 1$ mm), there exist hydrothermal waves in the pattern of curved spoke, and with the increase of *Ma* number, a single group of hydrothermal waves transform into two coexisting groups of hydrothermal waves that have different wave numbers and propagate in different directions; when the liquid pool is deep ($d \geq 5$ mm), Rayleigh-Bénard instability appears due to the influence of buoyancy, and the flow pattern of straight spoke appears in the entire surface region; when $2 \leq d \leq 4$ mm, hydrothermal waves and three-dimensional oscillatory flow exist simultaneously, in addition, hydrothermal waves are at the inner wall of the liquid pool, well, in the region near the hot wall, under the influence of hydrothermal waves, the generated pairs of longitudinal flow cells rotating counterclockwise propagate circumferentially at the same angular velocity of hydrothermal waves.

The study on thermocapillary convection of silicon melt in the rotating annular pool was completed by Shi et al. [53]. In the rotating annular pool, the propagating direction of the hydrothermal wave is opposite to the rotating direction of the liquid pool, which is because the flow field in the azimuthal direction generated by Corilois force supplied extra energy. In the rotating pool, under a certain *Ma* number, the wave number of azimuthal wave increases, and a branch comes out on the spiral wave at the inner wall; as *Ma* number is increased to a certain value, two groups of hydrothermal wave are generated, and the group with a smaller wave number propagates in the same direction as the rotating direction of the pool. Both numerical calculation and linear stability analysis show that, within a certain range of rotating velocity, the rotation of liquid pool will have influence on the steady axisymmetric thermocapillary convection, and even when the rotating velocity is very low, the influence on the instability of convection is significant. Li et al. [54] carried out in-depth study on the transition process of thermocapillary convection in the liquid pool rotating slowly. It is found from the results that, when the radial temperature gradient on the free surface is increased, two types of flow transition will occur. Under a certain rotating velocity, two-dimensional steady flow transits into the first type of hydrothermal wave, with further increase of temperature difference, the flow will transit into the second type of hydrothermal wave with fewer wave numbers. The critical values for the generation of hydrothermal waves and the critical region where these two types of hydrothermal wave transform to each other all depend on the rotating velocity. The critical temperature difference at which the second type transits into the first type and the critical temperature difference at which the first type transits into the second type have hysteresis, and in the critical region, there exists the phenomenon of having both types of hydrothermal wave. With the increase of rotating velocity of the annular pool, the propagating direction of the second type of hydrothermal wave transforms gradually from the opposite of the rotating direction of the liquid pool to the same of that. Afterwards, the higher the rotating velocity, the faster the propagating speed of the hydrothermal wave, therefore, the rotating velocity of the liquid pool decides the propagating direction of the hydrothermal wave.

3 Ground Experimental Study on Thermocapillary Convection

Through years of research, people have got fundamental understanding about the scientific laws of microgravity. The equation used to describe the fluid movement in microgravity environment is Navier-Stokes equation with the term of gravity neglected. The work has been focused on critical conditions, especially the influences of surface tension and the gradient of surface tension on the fluid interface as well as the contact angle effect on the liquid-solid interface. Perturbation analysis is usually adopted for some simple processes, that is, by applying a little linear perturbation to a steady basic state, to solve the perturbed linear system of equations, and analyze its linear instability. Some people also solve the process of instability by the energy method. At present, three-dimensional unsteady computational fluid dynamics method is widely used in the research on nonlinear dynamics problems.

Conducting small-scale ground experiments with small Bond number *Bo* is an effective method of simulation study on thermocapillary convection. *Bo* number is used to analyze the relative importance between the actions of gravity and surface tension. We can see from the expression of *Bo* number that, a small *Bo* number can be realized by the small fluid density, the small acceleration of gravity and the small size. The simulation experiment emphasizes the overall effect. The gravity still exists during the process, and it will cause deformations of free surface and introduce new characteristic scales. Thus, the scale of the ground experiment should be as small as possible, and the diagnostic technique of the experiment is required to be very high. Since the opportunity for the microgravity experiment in space is very rare, a large number of ground experiments with small *Bo* number are carried out as a preliminary study of the space experiment.

In recent years, the National Microgravity Laboratory carried out a lot of ground experimental studies on thermocapillary convection in the annular liquid pool. It is found that, under the action of horizontal radial temperature gradient, oscillations of internal temperature and free surface will occur. The critical conditions have been obtained. For the same silicone oil, the critical conditions of two kinds of oscillation have the same trend of change with the change of the thickness of liquid layer [55–57].

3.1 Experimental Model

An experimental system of buoyant-thermocapillary convection in the annular liquid pool is established to visualize flow behavior, as shown in Fig. 2. The annular pool is made of red copper with good thermal conductivity, and its inner radius is $Ri =$ 4 mm, outer radius is $Ro = 20$ mm, and depth is $d = 12$ mm. There is a resistance wire heating film in the central column for heating the fluid medium in the annulus. Six Peltier elements are attached to the external side of the liquid pool's outer wall for transferring the heat on the outer wall to the external environment, and keep the

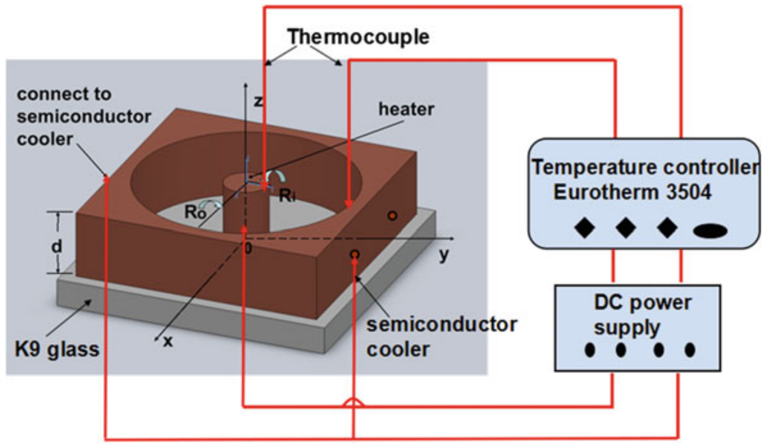

Fig. 2 Experimental system of Buoyant-thermocapillary convection

temperature of the cold end constant at a relative low level. The bottom of the pool is made of adiabatic material. The experimental media are KF96 1.5 and 2cSt silicone oil.

The Electric heating film and the Peltier elements are controlled to work according to the predetermined temperature control program through a DC power supply and a temperature controller, thus a horizontal temperature difference is generated in the annulus, and two thermocouples are used to monitor the temperature on the central column and the outer wall in real time. As the temperature difference between the two ends is increasing, the flow in the layer of silicone oil will transit from the steady state to the unsteady state, and the phenomenon of oscillation will appear.

3.2 Measurement System of Thermocapillary Convection

The temperature measurement system consists of T-type thermocouples, the nanovoltmeter, and the computer. In the experiment, T-type thermocouples are connected with the 2812A nanovoltmeter produced by Keithly to make up the temperature measurement system. The diameter of T-type thermocouple is 60 μm, and the soldered joint is 0.2 mm, one end is the measuring point and the other end is the cold end dipped in the ice water; the sensitivity of nanovoltmeter is as high as 1pV. The resolution of the whole temperature measurement system can reach 0.001 °C. The T-type thermocouples are put in the silicone oil directly, and the measured temperature signals are converted into voltage signals that can be recognized by the nanovoltmeter. Then the corresponding temperature values are calculated according to the relation between temperature and EMF (electromotive force), and they are recorded in the computer through the data acquisition instrument in real time.

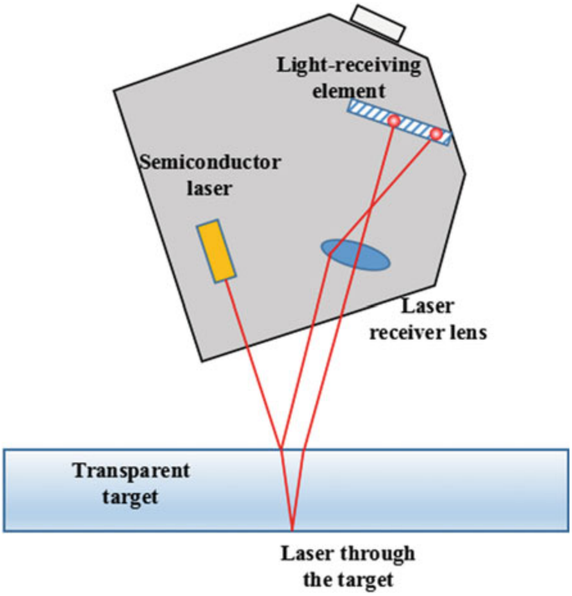

Fig. 3 Triangular measurement principle of the displacement sensor

The free surface oscillation measurement system consists of the LK-H080 high-precision laser displacement sensor produced by KEYENCE of Japan, the signal controller and the computer. The laser displacement sensor is based on triangular measurement principle, that is, the sensor calculates the distance to the object by focusing the light beam reflected from the object onto the light receiving element, as shown in Fig. 3.

The measurement of temperature distribution on the liquid surface uses the E60 thermal infrared imager produced by FLIR. It is set up right above the annular liquid pool and is focused on the fluid surface. The resolution of image is 320 × 240 pixels, the sensitivity of measurement is 0.05 °C, the precision of temperature measurement is ±2 °C, and the maximum acquisition rate can reach 30 frames/s. The imager can set parameters of radiance rate and working distance and convert thermal infrared graph into temperature automatically. Then the temperature data is output in the form of CVS table. We can also extract temperature data series with time of a few points in the radial or circumferential direction on the liquid surface for the analyses of frequency and amplitude.

We also used the optical shadow method to measure the temperature field inside the liquid layer. This method is a kind of flow visualization technique based on the principle that light beams are deflected in different directions in different flow states and they are focused or diverged to form an optical image. The light path diagram of the principle of shadow method is shown in the left part of Fig. 4. The laser beam passes through the beam expander and collimating lens to form parallel light; the

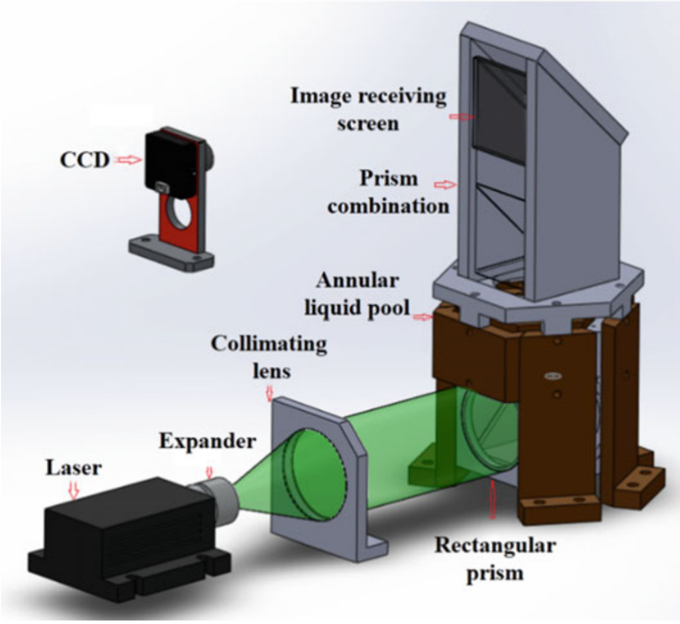

Fig. 4 The measurement system of shadow method

parallel lights totally reflected by the right angle prism that is installed right below the liquid pool, then it is projected onto the screen through the transparent bottom of the pool and the experimental medium, so the integral changing information of the fluid refractivity field (the corresponding temperature field) will be displayed on the screen in real time; videos are recorded by a CCD camera. Though the shadow method is usually used for qualitative visualization, since its pattern of light intensity has some regularity, in our analysis, we also extract a gray scale sequence at a certain point in the images to explain the change of temperature field.

3.3 Experimental Process and Results Analysis

In the experiment, the fluid in the annular liquid pool is 1.5 or 2cSt silicone oil, and the thickness of liquid layer increases from 0.8 to 3 mm with 0.25 mm per step. Various working conditions are experimentally studied. A T-type thermocouple is used to measure temperature oscillation signals at a single point in the liquid layer. With the increase of temperature difference, the internal temperature of fluid increases as well, and when the temperature difference reaches a critical value, the internal temperature of fluid starts to oscillate regularly, and the corresponding fluid flow transits from steady state to oscillatory convection. Figure 5 shows the original

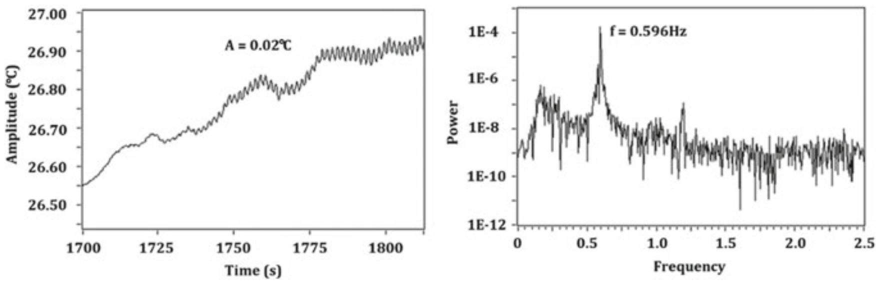

Fig. 5 Original temperature signals (left) and frequency spectrum analysis (right)

temperature signals (left) and frequency spectrum analysis (right) of 1.5cSt silicone oil. When the experiment time is at 1724 s, the temperature starts to oscillate, and the temperature difference is 16 °C at this time, then temperature oscillates regularly. The fundamental frequency in this stage is analyzed through fast Fourier transform (FFT). The fundamental frequency is 0.6 Hz, and the oscillation amplitude in this stage is 0.02 °C.

The free surface oscillation is an important characteristic in the transition process of thermocapillary convection. In the experiment, the free surface oscillation of thermocapillary convection in the annular liquid pool is measured with a displacement sensor simultaneously with the temperature measurement. Figure 6 shows the original displacement signals (left) and frequency spectrum analysis (right) of the measured point on the free surface in the working condition with 2 mm thick liquid layer of 1.5cSt silicone oil. At about 1710 s, when the displacement of the measured point on the free surface exceeds the threshold value, the displacement starts to oscillate regularly, and the temperature difference at this time is 16 °C. The fundamental frequency in this stage is analyzed through fast Fourier transform (FFT). The fundamental frequency is 0.6 Hz, and the oscillation amplitude is 1.09 μm.

The oscillation of free surface is the basic characteristic in the transition process of a dynamics system, and it is a physical quantity that is more sensitive than the oscillation of internal temperature of the fluid. With the increase of the temperature

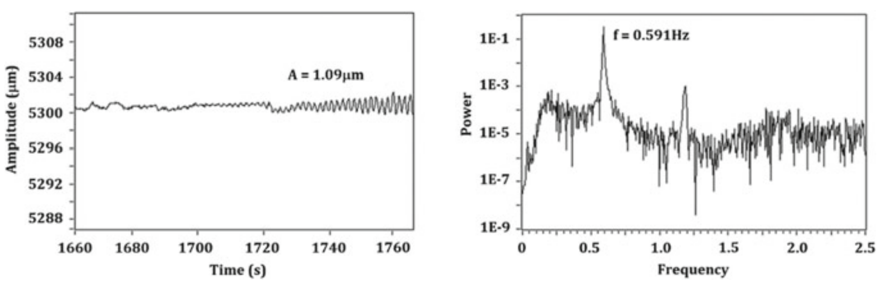

Fig. 6 Original displacement signals (left) and frequency spectrum analysis (right)

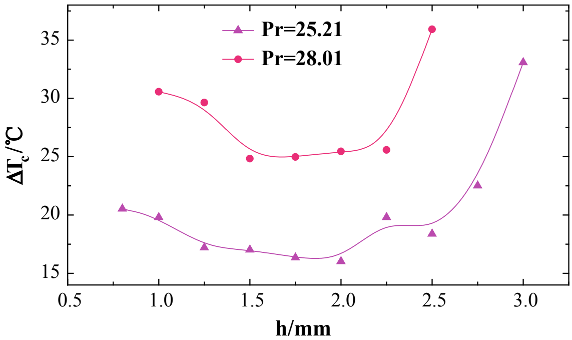

Fig. 7 Critical conditions

difference between the cold end and hot end, the fluid temperature changes as well, and when the critical temperature difference is reached, the free surface starts to oscillate regularly.

The critical values of temperature difference for the oscillation of buoyant-thermocapillary convection in 1.5cSt ($Pr = 25.21$) and 2cSt ($Pr = 28.01$) silicone oil with various thickness of liquid layer have been obtained. The critical curves are given as shown in Fig. 7. The critical temperature difference of buoyant-thermocapillary convection in 2cSt silicone oil is about 10°C higher than that in 1.5cSt silicone oil.

In the experiment of this study, a thermal infrared imager is used to capture the evolutionary process of the surface temperature field with the gradual increase of temperature difference between the inner and outer walls. The fluid media is 1cSt silicone oil with different thicknesses of liquid layer, and the purpose is to quantitatively observe the circumferential oscillation laws of temperature. It is found that a surface circumferential standing-wave mode exists in the transition of convection system in the annular liquid pool. With the increase of the radial temperature difference in the experiment, 7 standing-wave modes with different wave numbers ($m = 0$, 1, 5, 6, 7, 8, and 9), and a hydrothermal traveling-wave mode are roughly found, as shown in Fig. 8. The radial oscillation exists in the seven types of surface standing-wave modes, and the energy is transferred from the wave abdomen to the side wall. Meanwhile, the standing-wave mode is a two-dimensional oscillation flow; the traveling wave mode of hydrothermal wave is characterized by circumferential spiral-wave in one-way or two-way rotation; the wave number changes and temperature turning points are also different in the same heating process, under the different thicknesses of liquid layers. The first critical temperature difference is between 9 and 12°C. Direct transition to the hydrothermal wave only occurs in thin liquid layers ($h < 1.2$ mm, $Bo < 0.25$). When the liquid layer is larger than 1.2 mm, radial concentric circles oscillation ($m = 0$) will occur, and then circumferential standing waves will occur. The patterns observed in 1.5 mm thick liquid layer are the most abundant ($m = 0,9,6,8,7$), which may be because of the suited aspect ratio.

During the heating process of the model of buoyant-thermocapillary convection, the projected images by the flow visualization of shadow method are screened in full. In the experiment, the shadow images at different stages of the convection have been

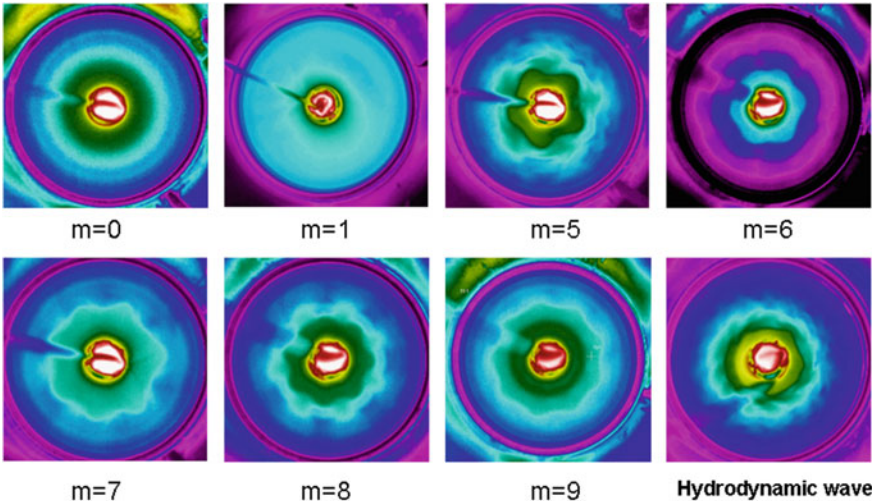

Fig. 8 Flow pattern transitions of Buoyant-thermocapillary convection, reprinted from Ref. [57], copyright 2016, with permission from Springer Nature

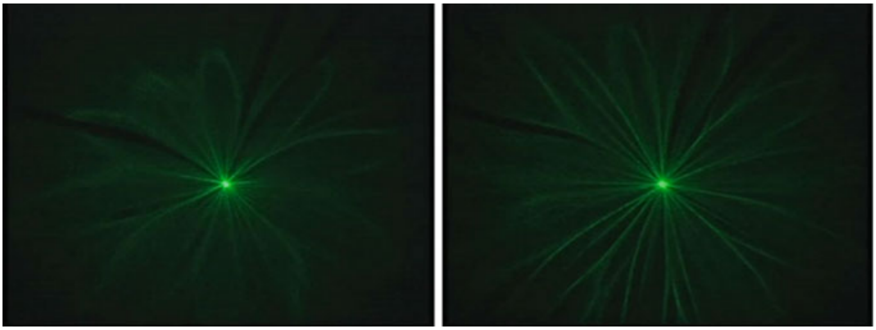

(a) 1D Hydrothermal Wave (b) 2D Hydrothermal Wave

Fig. 9 Shadow images of hydrothermal waves

captured. When the temperature difference is small, the distribution of light intensity of the shadow image is uniform. With the increase of temperature difference, the distribution of light intensity of the shadow image gradually transforms from a single uniform mode to a rotating pattern of two modes. One is a kind of spoke-shaped helicon waves that start from the source at the top left of the center propagating circumferentially in the opposite directions and at the same angular velocity to a centrosymmetric sink, as shown in Fig. 9a; the other is a kind of spoke-shaped helicon waves that start from the source propagating circumferentially to the sink and move forward in the radial direction, as shown in Fig. 9b.

By analysis in comparison with the temperature measurement method, it is found that, when the flow field is in static state or steady basic flow state, the radial temperature distribution is mostly linear with a small gradient because the distribution of temperature field is uniform. The temperature at each point in the space can be considered constant for a certain period of time, thus light can pass through evenly, and there is no local converging or diffusion; with the increase of temperature difference, the steady basic flow firstly transforms into the hydrothermal wave propagating circumferentially in one-dimensional rotation, i.e., 1D Hydrothermal Wave (HW1). The temperature on the concentric circumference is not the same any more, but in the distribution of helicon wave with alternate high and low temperature and rotating at a certain angular velocity. At this time, the temperature on the circumferential points change regularly with time, and there exists phase difference spatially, as a result, the change in refractivity field caused by the change in thermal field will change the path of light passing through, which will reflect the shadow image that is consistent with the propagation of hydrothermal wave. When the temperature difference is increased to a certain value, the radial oscillatory flow appears that has been in one-dimensional circumferential unsteady state, that is, the radial flow field shows an oscillatory flow propagating from inside to outside with the change of convective state, and this is called 2D Hydrothermal Wave (HW2). It can also be considered as a 2D oscillatory flow. The ununiformity and periodic change of temperature field can also be reflected in the shadow image through the deflection effect of radial light.

4 Experimental Study in Space on Thermocapillary Convection

Because the simulation experiment on the ground can hardly avoid the influence of gravity totally, it is necessary to carry out microgravity experiment in space. SJ-10 recoverable satellite for scientific experiments has been launched successfully on April 6th at 1:38 am. 19 experimental projects of microgravity science and space life science are carried out on SJ-10 this time, and the space experimental study on surface waves of thermocapillary convection is one of them.

4.1 Scientific Objectives

The scientific objectives of this project is to establish thermocapillary convection system in an annular (cylindrical) liquid pool in space, study destabilization laws and transition routes of thermocapillary convection, study volume ratio effect for the first time, and understand the instability and oscillation mechanism of thermocapillary convection.

4.2 Development of Payload

The space experimental payload has 8 systems, including the liquid pool system, the liquid storage and injection system, the temperature control system, the temperature measurement system with thermocouples, the thermal infrared imager, the displacement sensor, the CCD image acquisition system and the electrical control system, as shown in Fig. 10.

Thermocapillary flow system in the annular liquid pool is established by heating and cooling the fluid system in space (see Fig. 11). High-sensitivity thermocouples are used to measure the fluid temperature, the displacement sensor is used to measure deformations of liquid surface. By these methods together with the infrared imaging, the oscillation characteristics, transition conditions, transition processes and flow pattern transitions of thermocapillary convection are obtained. In the meantime, the problem of volume ratio effect is also studied, which cannot be carried out on the ground.

The technical parameters of the space model of annular liquid pool are same as that of the ground experiment model. During the space experiment, the liquid is injected into the pool from the liquid injection hole on the bottom of the pool. Because of the loss of gravity, the fluid will climb along the walls of the pool, so in order to maintain the fluid interface, the wedge-shaped edge is designed on the central column and the outer wall of the annulus at the same height. This realized the key technique for maintenance and control of the liquid surface in space.

The liquid storage and injection system consists of the electric motor, liquid cylinder, transmission rod, pipeline and solenoid valve as shown in Fig. 12. Before the space experiment, the fluid is stored in the liquid cylinder, and at the beginning of the experiment, the fluid is injected into the annular liquid pool by the stepper motor to form the experimental fluid system. M-227 motor produced by PI of Germany is selected in this experiment, and it is driven by C-863 controller. The transmission rod is designed to connect the stepper motor and the piston of liquid cylinder.

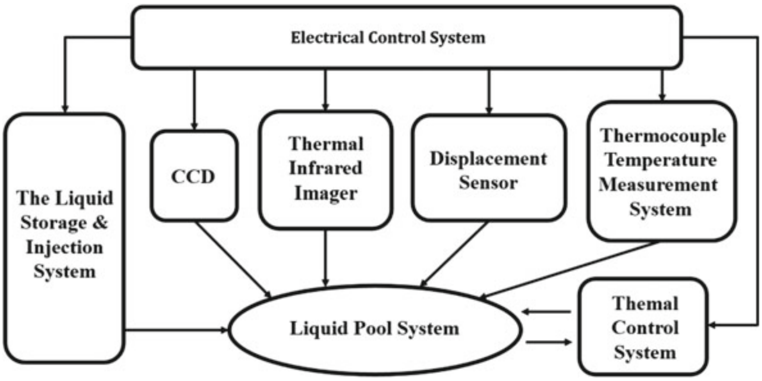

Fig. 10 The composition of payload

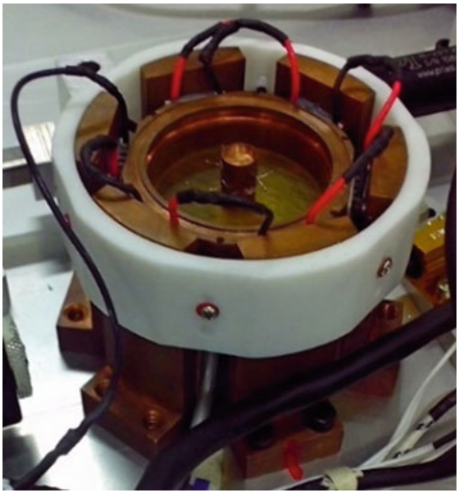

Fig. 11 The annular liquid pool, reprinted from Ref. [57], copyright 2016, with permission from Springer Nature

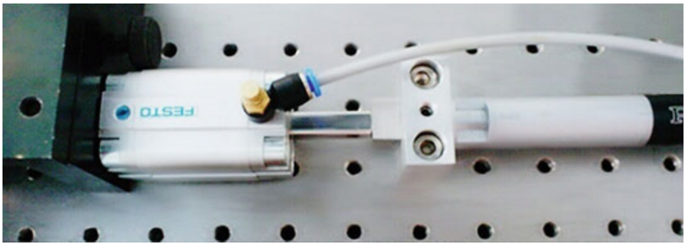

Fig. 12 The liquid storage and injection system, reprinted from Ref. [57], copyright 2016, with permission from Springer Nature

The liquid cylinder, pipeline and the solenoid valve are all products of FESTO of Germany. The model of liquid cylinder is ADVU-40-25-P-A. Its internal diameter is 40 mm, and its effective movement region is 25 mm. The model of solenoid valve is MSFG-12-0D. The transmission of experimental working fluid between the liquid pool and the liquid cylinder is controlled through opening and breaking of the solenoid valve. In the process of liquid loading, the negative pressure injection method is used, which ensures that there is no air bubble in the liquid model in the space experiment. This is also one of the key techniques in our project.

The temperature control system mainly includes high temperature sensor, low temperature sensor and ambient temperature sensor, the heating column and Peltier elements. Each part of the temperature control system is under the unified control and management of the electric control system. The temperature on the inner wall and the outer wall of the liquid pool is adjusted by PID control to ensure the temperature difference between the two ends of fluid within the required range of the experiment.

The image acquisition system includes a CCD camera and LED light source. The CCD camera is the model WAT-230VIVID produced by WATTEC of Japan, with effective pixels of 752 × 582, and analog video outputs. The LED light source selects hemispherical high-brightness LEDs, and the model is 1025MW7C. In the experiment, two LEDs are connected in series and parallel with another two in series, with the protecting resistor connected in series, to make sure the light source can work reliably and safely.

Two methods of temperature measurement are adopted in this experiment. One is using thermocouple sensors that measure the temperature directly and transform temperature signals into EMF signals. This thermocouple has a measuring range of −40 to +125 °C, and a sensitivity of 0.05 °C. The other technique of temperature measurement is using the thermal infrared imager to measure the temperature distribution on the liquid surface of thermocapillary convection. The thermal infrared imaging technology uses various detective sensors to receive infrared radiation from the object, then processes the photoelectric information, and finally displays the temperature distribution of fluid surface by digits, signals and images. HL-C1 ultra-high-speed laser displacement sensor produced by Panasonic of Japan is selected to measure deformations of fluid surface. It can realize the ultra-high-precision measurement with a high sampling speed of 100 μs, resolution of 1 μm, and linearity of ±0.1% F.S.

The computer control system implements the ON/OFF operations for the whole experimental device, receives the 28 V power supply from the payload manager, and uniformly provides and distributes power supplies to each subunit in the whole device; it injects instructions and uploads engineering parameters and scientific data through the communication ports; it manages equipment such as stepper motor controller, CCD camera, LED light source, thermal infrared imager, displacement sensor, solenoid valve, and so on; according to the ambient temperature and the temperature measurement conditions of high temperature and low temperature sensors, it controls the heating column and Peltier elements to reach the temperature difference requirement and collects and downloads temperature signals in real time.

This project is for the study on volume ratio effect and transition problems of pure thermocapillary convection in the microgravity environment in space. For thermocapillary convection system in an annular liquid pool, the study on volume ratio effect has to be carried out in the microgravity environment in space; about the problem of oscillation transition, a new phenomenon has been found in our ground experiment, that is, after the onset of oscillation, the oscillation disappears with the increase of temperature difference, and this has not been discovered in any other's experimental studies, and whether it is an inherent characteristic of thermocapillary convective oscillation in the annular liquid pool or due to the influence of gravity needs to be verified in the space experiment; in addition, it is found in the ground experiment that multiple oscillation frequencies exist simultaneously, and they increase with the increase of temperature difference, and this phenomenon of increasing fundamental frequencies also needs to be further studied in the space experiment. Therefore, the study on volume ratio effect and transition problems of pure thermocapillary flow system reflects the innovative idea of space experiments. The internal structure and the external appearance of the experiment case are shown in Fig. 13.

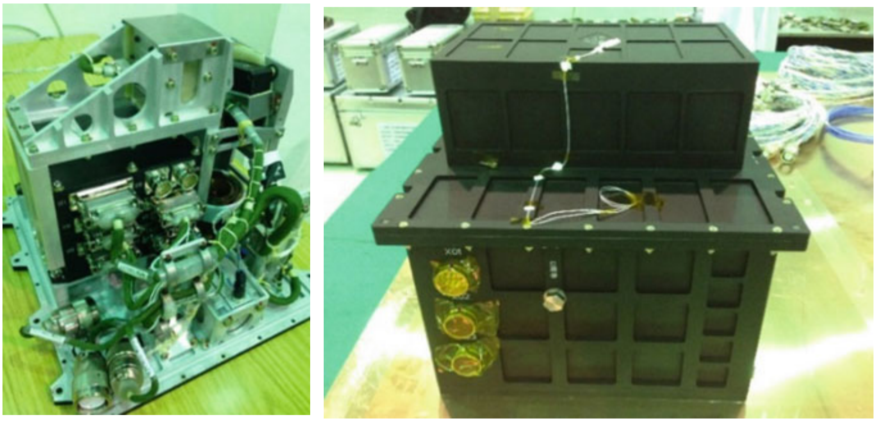

(a) The internal structure (b) The payload box

Fig. 13 The internal structure and external appearance of the payload

4.3 Preliminary Results of the Space Experiment

In this space mission, 23 space experiments on surface waves of thermocapillary convection have been completed, including 13 times and 10 times respectively before and after the separation of orbit capsule and reenter capsule; 17 experiments used the linear heating mode and 6 experiments used the step heating mode; the volume ratio is 0.363–1.220; the max temperature difference is 25 °C, 29 °C, 31 °C, 32 °C, 34 °C, 35 °C, and 40 °C respectively; the heating rate includes 0.5 °C/min and 1.0 °C/min. Figure 14 shows the picture of fluid model captured by CCD during the experimental process in space and the temperature control curve, which indicates that the liquid has been injected successfully in the microgravity environment and the temperature has been controlled successfully.

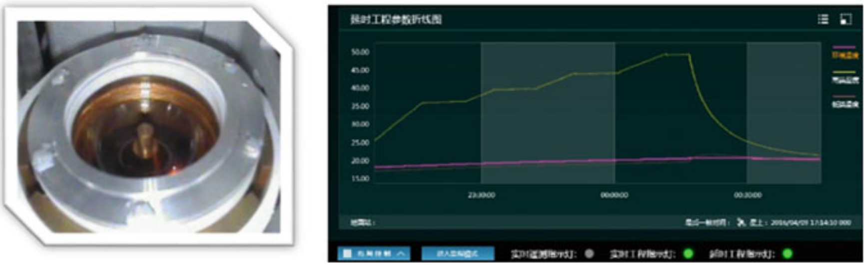

(a) The space experimental model (b) The temperature control curve

Fig. 14 The fluid model of space experiment and the temperature control curve

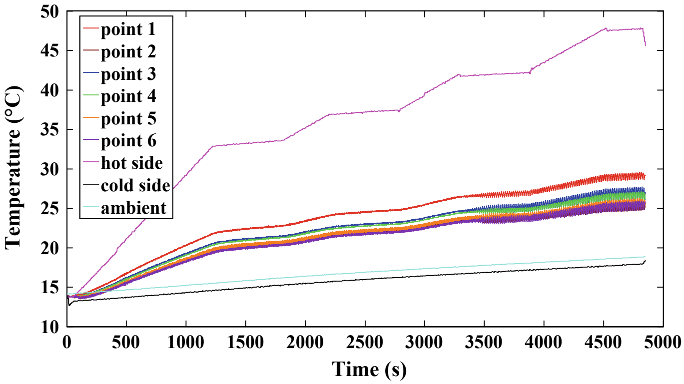

Fig. 15 The original temperature data in the space experiments

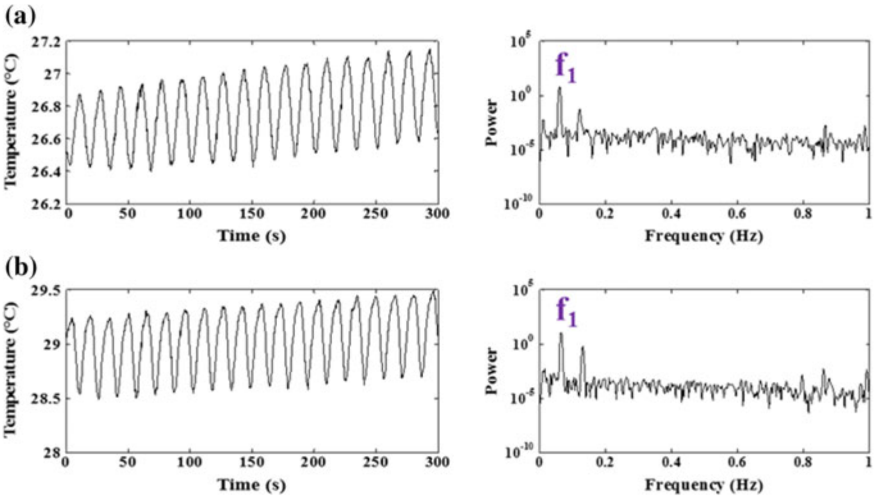

Fig. 16 The temperature oscillation and frequency spectrum analysis

The phenomenon of temperature oscillation is found according to the measuring results of thermocouples, as shown in Fig. 15. The oscillation frequencies are significantly lower than that measured in the ground experiments, with a difference of almost an order of magnitude, as shown in Fig. 16. The analysis shows that, the critical curves are separated into two branches. When the volume ratio is less than about 0.65, the critical temperature difference increases with the increase of volume ratio, and when the volume ratio is larger than about 0.65, the critical temperature difference decreases with the increase of volume ratio, as shown in Fig. 17. The quasi-periodic bifurcation and the period-doubling bifurcation have been discovered.

From the comparison between deformation measurements of liquid surface by the displacement sensor and the fluid temperature measurements, it is found that the

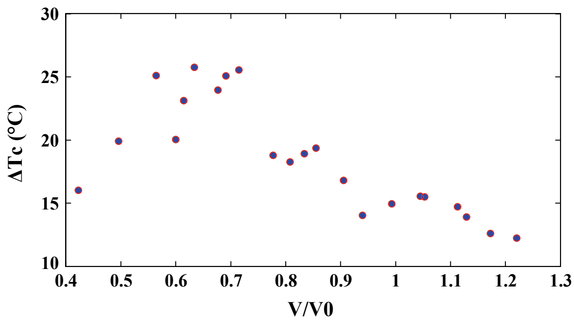

Fig. 17 The critical conditions

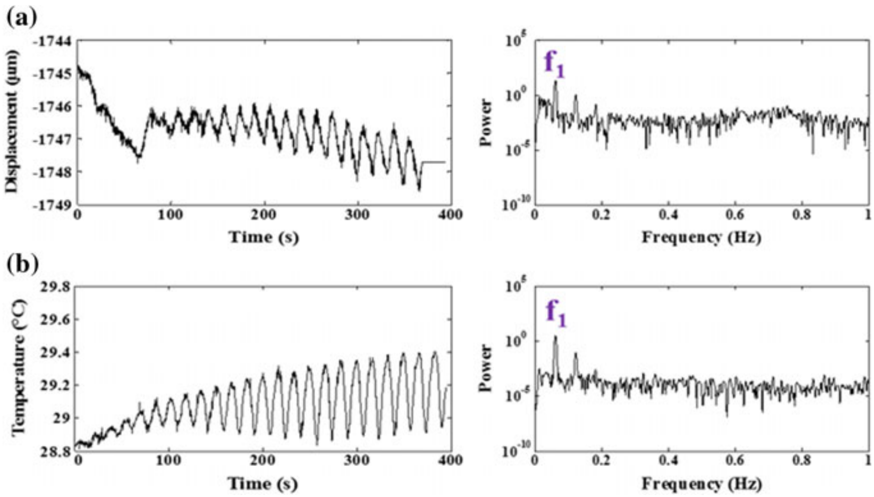

Fig. 18 The comparison between liquid surface oscillation (**a**) and fluid temperature oscillation (**b**)

liquid surface and the temperature start to oscillate simultaneously with the same oscillation frequency, as shown in Fig. 18.

The infrared measurement results of temperature distribution on the fluid surface at 23 working conditions with various volume ratios have been obtained in the space experiments. It is found that, the temperature on the fluid surface starts the axial oscillation first and transits to circumferential rotation, and then transits to the coexisting mode of axial oscillation and circumferential rotation together. This means that, thermocapillary convection transits from steady state to standing wave mode and then to travelling wave mode, and finally to the coupled mode of standing wave and travelling wave. Two oscillation modes with wave numbers of 3 and 4 have been found, as shown in Fig. 19. A large number of space experimental results have been processed, and more research results have been reported [58–60].

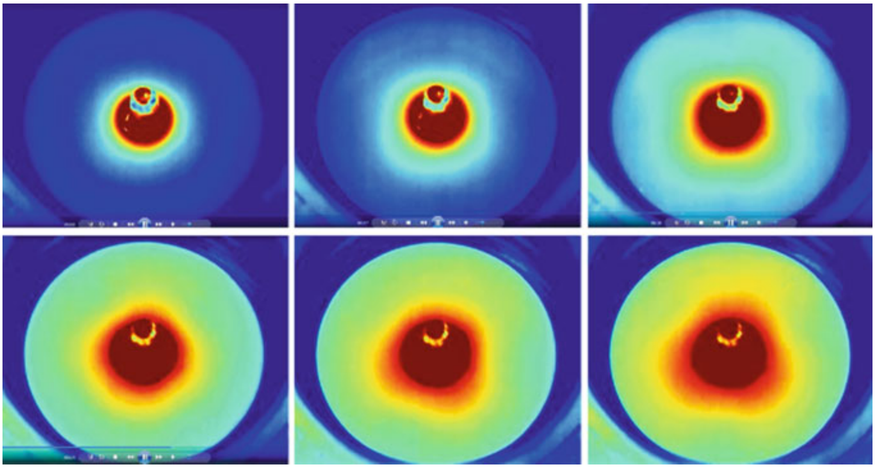

Fig. 19 The transition from wave number $m = 4$ to $m = 3$

5 Summary

This paper introduces the ground experiments and the space experiments on the thermocapillary convection in an annular liquid pool. In the ground experiments, thermocapillary convections with different depths (0.8 to 3 mm) are studied. The critical temperature difference of 2cSt silicone oil is about 10°C higher than that in 1.5cSt silicone oil. The transition from steady state to oscillatory convection is observed by the thermal couples, displacement sensor, infrared image and shadow graph. In the space experiments, thermocapillary convection with different volume ratio are studied. The critical condition is sensitive to the variation of volume ratio, which the critical curve can be divided into two branches. Due to the effect of buoyancy, the oscillatory convection only presents in a very thin layer in the ground experiments. However, in the space experiments, the oscillatory convection occurs in the deep layer (12 mm) with different surface configurations. It is found that thermocapillary convection transits from steady state to standing wave mode and then to travelling wave mode, and finally to the coupled mode of standing wave and travelling wave. In the future, we will give an in-depth analysis on the space experiments to give a better understand the characteristic, transition and nonlinear dynamic of the oscillatory thermocapillary convection.

Acknowledgements This project was funded by the National Natural Science Foundation of China (U1738116), and the Strategic Priority Research Program on Space Science of Chinese Academy of Sciences—SJ-10 Recoverable Scientific Experiment Satellite (XDA04020405 and XDA04020202-05).

The development of this space experimental payload got assistance from Astronaut Research and Training Center and Shenyang Zhixing Science and Technology Company Limited etc. The related experimental results and processing results of space experimental data obtained by the staffs and students of our project group are presented in this paper. Appreciations to all of them.

References

1. Cockayne B, Gates MP (1967) Growth striations in vertically pulled oxide and fluoride single crystals. J Mater Sci 2(2):118–123
2. Kobayashi N (1978) Computational simulation of the melt flow during Czochralski growth. J Cryst Growth 43(3):357–363
3. Kobayashi N, Wilcox WR (1982) Computational studies of convection due to rotation in a cylindrical floating zone. J Cryst Growth 59(3):616–624
4. Langlois WE, Shir CC (1977) Digital simulation of flow patterns in the Czochralski crystal-pulling process. Comput Methods Appl Mech Eng 12(2):145–152
5. Langlois WE (1985) Buoyancy-driven flows in crystal-growth melts. Annu Rev Fluid Mech 17(1):191–215
6. Ostrach S (1982) Low-gravity fluid flows. Annu Rev Fluid Mech 14(1):313–345
7. Napolitano LG, Monti R, Russo G (1984) Some results of the Marangoni free convection experiment. In: Materials science under microgravity. Results of Spacelab 1, vol 1, pp 15–22
8. Schmidt RJ, Milverton SW (1935) On the instability of a fluid when heated from below. Proc R Soc London Ser A Math Phys Sci 152(877):586–594
9. Smith MK, Davis SH (1983) Instabilities of dynamic thermocapillary liquid layers. Part 1. Convective instabilities. J Fluid Mech 132:119–144
10. Hu W et al (2010) Introduction to microgravity science. Science Press, Beijing (in Chinese)
11. Hashim I, Sarma W (2007) On oscillatory Marangoni convection in a rotating fluid layer subject to a uniform heat flux from below. Int Commun Heat Mass Transfer 34:225–230
12. Nepomnyashchy AA, Simanovskii IB, Braverman LM (2001) Stability of thermocapillary flows with inclined temperature gradient. J Fluid Mech 442:141–155
13. Kats-Demyanets V, Oron A, Nepomnyashchy AA (1997) Linear stability of a tri-layer fluid system driven by the thermocapillary effect. Actaastronautica 40(9):655–661
14. Ermakov MK, Ermakova MS (2004) Linear-stability analysis of thermocapillary convection in liquid bridges with highly deformed free surface. J Cryst Growth 266(1):160–166
15. Shiratori S, Kuhlmann HC, Hibiya T (2007) Linear stability of thermocapillary flow in partially confined half-zones. Phys Fluids (1994–present) 19(4):044103
16. Xu B, Ai X, Li BQ (2007) Stabilities of combined radiation and Rayleigh–Bénard–Marangoni convection in an open vertical cylinder. Int J Heat Mass Transf 50(15):3035–3046
17. Li MW, Zeng DL, Zhu TX (2002) Instability of the Marangoni convection in a liquid bridge with liquid encapsulation under microgravity condition. Int J Heat Mass Transf 45(1):157–164
18. Guo WD, Narayanan R (2007) Onset of Rayleigh–Marangoni convection in a cylindrical annulus heated from below. J Colloid Interface Sci 314(2):727–732
19. Hoyas S, Herrero H, Mancho AM (2004) Thermocapillar and thermogravitatory waves in a convection problem. Theoret Comput Fluid Dyn 18(2–4):309–321
20. Zhu P, Duan L, Kang Q (2013) Transition to chaos in thermocapillary convection. Int J Heat Mass Transf 57:457–464
21. Zhu P, Zhou B, Duan L, Kang Q (2011) Characteristics of surface oscillation in thermocapillary convection, Exp Thermal Fluid Sci 35:1444–1450
22. Jiang H, Duan L, Kang Q (2017) A peculiar bifurcation transition route of thermocapillary convection in rectangular liquid layers. Exp Thermal Fluid Sci 88:8–15
23. Jiang H, Duan L, Kang Q (2017) Instabilities of thermocapillary–buoyancy convection in open rectangular liquid layers, Chin Phys B 26(11):114703
24. Wang J, Di W, Duan L, Kang Q (2017) Ground experiment on the instability of buoyant-thermocapillary convection in large-scale liquid bridge with large Prandtl number. Int J Heat Mass Transf 108:2107–2119

25. Wang J, Duan L, Kang Q (2017) Oscillatory and chaotic buoyant-thermocapillary convection in the large-scale liquid bridge, Chin Phys Lett 34(7):074703
26. Tang ZM, Hu WR (1995) Fractal feature of oscillatory convection in the half-floating zone. Int J Heat Mass Transfer 38(17):3295–3303
27. Li K, Xun B, Hu WR (2016) Some bifurcation routes to chaos of thermocapillary convection in two-dimensional liquid layers of finite extent. Phys Fluids 28:054106
28. Kamotani Y, Lee J, Ostrach S (1992) An experimental study of oscillatory thermocapillary convection in cylindrical containers. Phys Fluids A 4:955–962
29. Kamotani Y, Chang A, Ostrach S (1994) Effects of heating mode on steady antisymmetric thermocapillary flows in microgravity. Heat Transf Microgravity Systems Trans ASME 290:53–59
30. Kamotani Y, Ostrach S, Pline A (1995) A thermocapillary convection experiment in microgravity. J Heat Trans-T ASME 117:611–618
31. Kamotani Y, Ostrach S, Pline A (1994) Analysis of velocity data taken in surface tension driven convection experiment in microgravity. Phys Fluids A 6:3601–3609
32. Kamotani Y, Ostrach S, Masud J (2000) Microgravity experiments and analysis of oscillatory thermocapillary flows in cylindrical containers. J Fluid Mech 410:211–233
33. Kamotani Y, Ostrach S, Pline A (1998) Some temperature field results from the thermocapillary flow experiment aboard USML-2 spacelab. Adv Space Res 22:1189–1195
34. Kamotani Y (1997) Surface tension driven convection in microgravity. Adv Astronaut Sci 96:487–499
35. Kamotani Y, Masud J, Lee JH, Pline A (1995) Oscillatory convection due to combined buoyancy and thermocapillarity. AIAA-paper 95-0817
36. Kamotani Y, Masud J, Pline A (1996) Oscillatory convection due to combined buoyancy and thermocapillarity. J Thermophys Heat Tr 10:102–108
37. Lin J, Kamotani Y, Ostrach S (1995) An experimental study of free surface deformation in oscillatory thermocapillary flow. Acta Astronaut 34:525–536
38. Renaud L, Gustav A, Henrik A (2001) Experimental and numerical investigation of nonlinear thermocapillary oscillations in an annular geometry. J Mech B Fluids 20:771–797
39. van der Vorst HA (1992) Bi-CGSTAB: a fast and smoothly converging variant of Bi-CG for the solution of nonsymmetric linear systems. SIAM J Sci Stat Comput 13:631–644
40. Li YR, Peng L, Akiyama Y, Imaishi N (2003) Three-dimensional numerical simulation of thermocapillary flow of moderate Prandtl number fluid in an annular pool. J Crystal Growth 259:374–387
41. Li YR, Imaishi N, Peng L, Wu SY, Hibiya T (2004) Thermocapillary flow in a shallow molten Silicon pool with Czconfiguration. J Crystal Growth 266:88–95
42. Li YR, Imaishi N, Azami T, Hibiya T (2004) Three-dimensional oscillatory flow in a thin annular pool of Silicon melt. J. Crystal Growth. 260:28–42
43. Sim BC, Kim WS, Zebib A (2004) Axisymmetric thermocapillary convection in open cylindrical annuli with deforming interfaces. J Heat Mass Transfer 47:5365–5373
44. Sim BC, Zebib A (2004) Thermocapillary convection in cylindrical liquid bridges and annuli. CR Mecanique 332:473–486
45. Schwabe D, Benz S, Cramer A (1999) Experiment on the multi-roll-structure of thermocapillary flow in side-heated thin liquid layers. Adv Space Res 24(10):1367–1373
46. Benz S, Schwabe D (2001) The three-dimensional stationary instability in dynamic thermocapillary shallow cavities. Exp Fluids 31:409–416
47. Schwabe D, Benz S (2002) Thermocapillary flow instabilities in an annulus under microgravity results of the experiment MAGIA. Adv Space Res 29:629–638
48. Schwabe D (2002) Buoyant-thermocapillary and pure thermocapillary convective instabilities in Czochralskisystems. J Crystal Growth 237–239:1849–1853
49. Li YR, Peng L, Wu SY (2004) Thermocapillary convection in a differentially heated annular pool for moderate Prandtl number fluid. Int J Therm Sci 43:587–593
50. Li YR, Imaishi N, Azami T et al (2004) Three-dimensional oscillatory flow in a thin annular pool of silicon melt. J Crystal Growth 260:28–42

51. Shi WY, Imaishi N (2006) Hydrothermal waves in differentially heated shallow annular pools of silicone oil. J Crystal Growth 290:280–291
52. Peng L, Li YR, Shi WY (2007) Three-demensional thermocapillary-buoyancy flow of silicone oil in a differentially heated annular pool. J Heat Mass Transfer 50:872–880
53. Shi WY, Ermakov MK, Imaishi N (2006) Effect of pool rotation on thermocapillary convection in shallow annular pool of silicone oil. J Crystal Growth 294:474–485
54. Li YR, Xiao L, Wu SY (2007) Effect of pool rotation on flow pattern transition of silicon melt thermocapillary flow in a slowly rotating shallow annular pool. Int J Heat Mass Transfer
55. Zhang L, Duan L, Kang Q (2014) An experimental research on surface oscillation of buoyant-thermocapillary convection in an open cylindrical annuli. Acta Mechanica Sinica 30(5):681–686
56. Zhang D, Duan L, Kang Q (2016) Critical condition of buoyancy—thermal capillary convection oscillations in annular liquid pool. Mechanics and practice (in Chinese)
57. Kang Q, Duan L, Zhang L, Yin Y, Yang J, Hu W (2016) Thermocapillary convection experiment facility of an open cylindrical annuli for SJ-10 satellite. Microgravity Sci Technol 28:123–132
58. Kang Q, Jiang H, Duan L, Zhang C, Hu W (2019) The critical condition and oscillation - transition characteristics of thermocapillary convection in the space experiment on SJ-10 satellite. Int J Heat Mass Transf 135:479–490
59. Kang Q, Wang J, Duan L, Su YY, He JW, Wu D, Hu WR (2019) The volume ratio effect on flow patterns and transition processes of thermocapillary convection. J Fluid Mech 868:560–583
60. Kang Q, Wu D, Duan L, He J, Hu L, Duan L, Hu W (2019) Surface configurations and wave patterns of thermocapillary convection onboard the SJ10 satellite. Phys Fluids 31:044105